

# Supplement to “ECB monetary policy surprises: identification through cojumps in interest rates”

Lars Winkelmann<sup>a</sup>, Markus Bibinger<sup>b</sup>, Tobias Linzert<sup>c</sup>

<sup>a</sup>*Department of Economics, Freie Universität Berlin*

<sup>b</sup>*Department of Mathematics, Humboldt-Universität Berlin*

<sup>c</sup>*European Central Bank*

January 22, 2015

## Finite sample analysis of the statistical procedure

This supplementary material to Winkelmann et al. (2015) illuminates the accuracy of our statistical approach in finite samples. We shall demonstrate that the methods perform well in realistic scenarios with non-synchronous observations and with locally varying observation frequencies. To this end, we simulate noisy observations of semimartingales discretely recorded on  $[0, 1]$  at times  $t_i^{(q)}, i = 0, \dots, T^{(q)}, q = 1, 2$ , with  $T^{(1)} = 10000$  and  $T^{(2)} = 5000$ . Given the fixed number of observations, we generate the random observation times for both processes according to a law which mimics a typical evolution of intraday trading activity as for our data application and which is at the same time in accordance with our theoretical assertions.<sup>1</sup> The distribution of observation times is visualized in Figure 1.

In this Monte Carlo experiment, we simulate stochastic volatilities

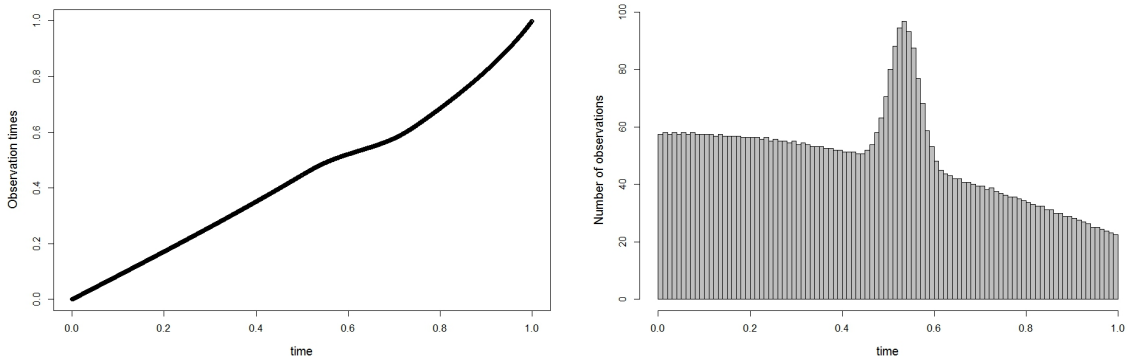
$$\sigma_t^{(q)} = \left( \int_0^t \frac{1}{2} dW_s^{(q)} + \int_0^t \frac{1}{2} dW_s^{(q),\perp} \right) \cdot 0.1 \left( 1 - t^{\frac{1}{3}} + 0.5t^2 \right), t \in [0, 1], q = 1, 2, \quad (1)$$

comprising leverage, a typical intra-day shape (second factor) as well as random fluctuations.  $W^{(q),\perp}, q = 1, 2$ , are two independent standard Brownian motions independent of  $W^{(q)}$ , the Brownian motions driving  $X_t^{(q)} = X_0^{(q)} + \int_0^t \sigma_s^{(q)} dW_s^{(q)} + J_t^{(q)}, q = 1, 2$ . We set  $\rho = 1/2$  as correlation of  $W^{(1)}$  and  $W^{(2)}$  such that the resulting integrated covolatility is positive. Discrete recordings  $Y_i^{(q)} = X_i^{(q)} + \varepsilon_i^{(q)}$  are diluted with i.i.d. Gaussian errors with expectations zero and standard deviations  $\eta^{(1)} = \eta^{(2)} = 0.001$  of realistic magnitude. The

---

<sup>1</sup>We utilize a pdf  $\propto \cos((3/16)\pi t) + (1/3) \exp(-(t - 0.535)^2 \cdot 500)$ , the associated cdf  $F$  and its numerical inverse  $F^{-1}$  which satisfies  $t_i^{(q)} \stackrel{d}{=} F^{-1}(i/T^{(q)})$ .

Figure 1: Distribution of simulated intraday observation times.



*Note: Left plot depicts observation times  $t_i^{(2)}, i = 0, \dots, T^{(2)}$ , in one simulation (y-axis) against intraday clock (x-axis). Right plot gives empirical distribution of observation times for one simulation (100 bins).*

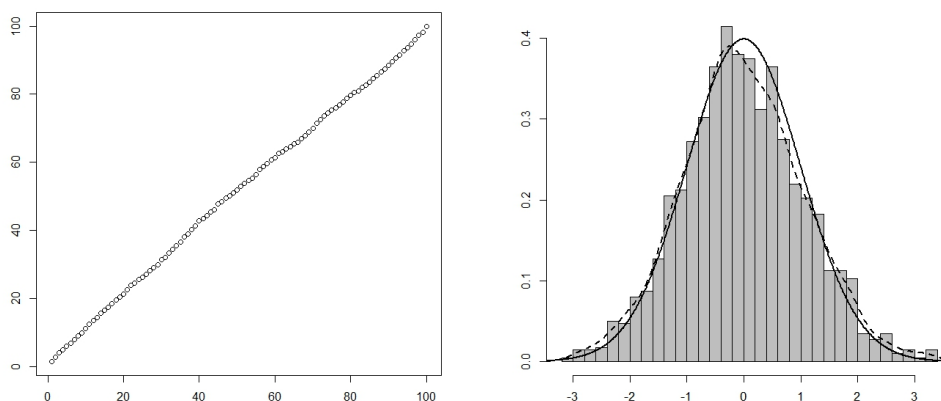
spectral estimators have been thoroughly investigated in Monte Carlo studies by Bibinger and Winkelmann (2015) and Bibinger et al. (2014), while our main focus here is on the precision of the test. We employ the block-wise adapted time-varying thresholding procedure, i.e.  $\hat{u}_k = 2 \log(h^{-1}) h \sigma_k^{(1,2)}$ , with  $k = 0, \dots, h^{-1} - 1$ , and  $\sigma_k^{(1,2)}$  the pilot estimator of the block-wise covolatility. We fix  $J = 30$  as spectral cut-off frequency which is large enough such that higher frequencies are negligible.

First, the number of blocks is set  $h^{-1} = 33$ , which equals our choice of 20 minutes intervals in the data analysis of Winkelmann et al. (2015). Below, we consider smaller blocks as well and shall see that the results are reasonably robust against different block lengths and that 33 is an adequate choice.

In the sequel, we visualize the empirical size and power of the test by comparing empirical against theoretical asymptotic percentiles, i.e. the  $q/100$ -quantiles for  $q = 1, \dots, 99$  of the theoretical Gaussian limit distribution under the hypothesis. First, we simulate 10000 Monte Carlo iterations under the hypothesis with no cojumps to reveal the test's finite sample size. Idiosyncratic jumps are implemented according to a compound Poisson process with one expected jump in each component and jump heights from a normal distribution  $N(0.05, 0.0001) \cdot U$ , where  $U$  determines the direction of a jump by taking values  $\{-1, 1\}$ , each with probability 1/2. Figure 2 visualizes the size of the test in the Monte Carlo experiment. The results confirm that the finite-sample behavior is very well-predicted by the asymptotic results.

Next, consider the finite-sample power. The same graphics as in Figure 2 portray the power in case that we simulate under the alternative. For this purpose we simulate 10000 iterations from the above scenario, but with one cojump occurring in each run at uniform

Figure 2: Size of the cojump test in Monte Carlo.



*Note: Left plot depicts percentage of realized test statistics (y-axis) smaller or equal the theoretical percentiles of theoretical limit distribution (x-axis). Right plot gives empirical distribution of test statistics, dashed line theoretical limit and solid line kernel density estimate.*

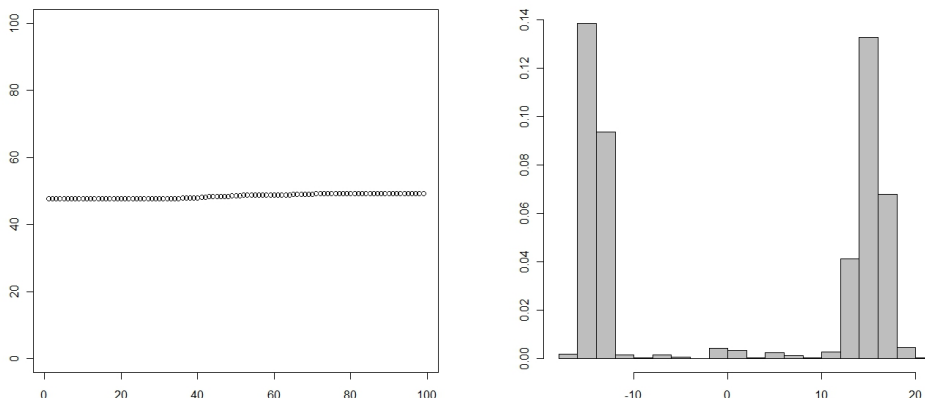
on  $[0, 1]$  distributed time. In each component we generate jumps  $N(0.05, 0.0001) \cdot U$ . This results with equal probability either in a unidirectional cojump (level shift), or a cojump with opposite directions (rotation).

Figure 3 shows a finite-sample power very close to 1 for this Monte Carlo experiment. About one half of the iterations with unidirectional cojumps result in large positive values of the test statistic while cojumps in opposite directions lead to negative test statistics with large absolute values. The configuration appears to be realistic with moderate average jump sizes as in this setup for a cojump at  $t$  we have  $|\Delta J_t^{(1)}| \approx |\Delta J_t^{(2)}| \approx 60 \text{ Mean}(|\Delta_i X^{(q)}|)$ ,  $q = 1, 2$ , such that the jumps are ca. 60 times the average increment from the continuous motion (which are in practice often equal to smallest unit).

Finally, we apply the test to simulated data with cojumps of even smaller size, distributed according to  $N(0.02, 0.0001) \cdot U$ , to further explore the limits of feasibility of the truncation methodology. We disclose the properties of our test in this framework in Figure 4. In this setting  $|\Delta J_t^{(1)}| \approx |\Delta J_t^{(2)}| \approx 20 \text{ Mean}(|\Delta_i X^{(q)}|)$ ,  $q = 1, 2$ , the jump size is comparable to the magnitude of the threshold and hence only in about 92% of the 10000 iterations the cojumps are recovered based on the truncation principle. Furthermore, since the continuous part of covariation is always positive, in this configuration opposite cojumps are even harder to detect via thresholding which produces a slight asymmetry in Figure 4.

Naturally the power is not as high as before. Still, the performance of the test gives reasonable results. Figure 5 shows the simulated noisy paths of one iteration in which the jumps are still visible - which is not always the case under this configuration. For

Figure 3: Power of the cojump test in Monte Carlo (1).



*Note: Left plot depicts percentage of realized test statistics (y-axis) against theoretical percentiles of the limit distribution under the hypothesis (x-axis). Right plot gives empirical distribution of test statistics.*

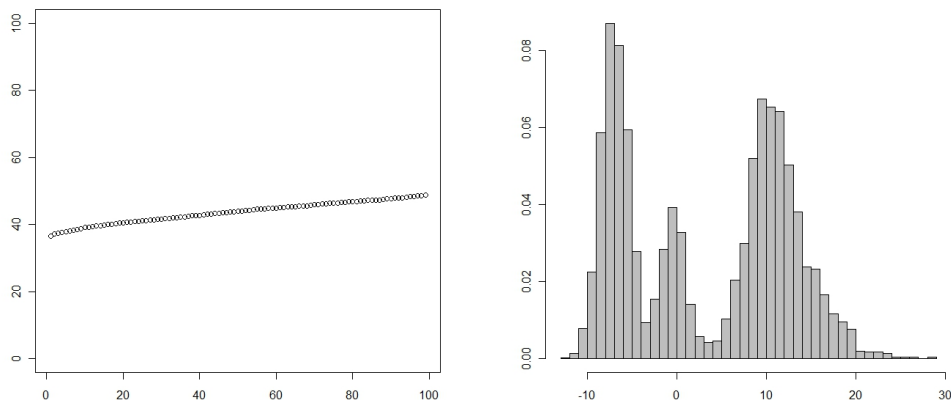
convenience the cojump arrival time is marked by the dashed lines. This examples intends to shed a light on what is possible in practice and grasp insight about the capabilities to detect cojumps by truncation (in the depicted example the cojump is clearly detected from the spectral statistics).

We repeat the Monte Carlo study using  $h^{-1} = 100$  blocks instead of  $h^{-1} = 33$ . This corresponds to time intervals of ca. 5 minutes instead of 20 minutes in the data analysis. The number of observations (in mean) per block can easily be seen in Figure 1 as we use there 100 bins to illustrate the law of observation times. Although the numbers per block are below 100 for most blocks, we are still in a range where the statistical methods work reasonably well.

The empirical size and power for alternatives with cojumps from a  $N(0.05, 0.0001) \cdot U$ -law and a  $N(0.02, 0.0001) \cdot U$ -law, respectively, are presented in Figure 6. The results show that the test performs quite well also for  $h^{-1} = 100$ , though the accuracy of the fit by the asymptotic results is slightly lower than before for  $h^{-1} = 33$ . From extensive simulations using different configurations, we can report that the test performs well in a broad range for  $h$ . Only in case that we select  $h$  even smaller, such that much less than 100 observations fall within one block, the size and power deteriorate significantly. On the other hand, taking  $h^{-1}$  much smaller than 33, the power (for moderate cojump sizes) also deteriorates as under low time resolution the separation of covolatility and cojumps gets less sharp.

To sum up, the Monte Carlo example demonstrates the high practical value of the hybrid

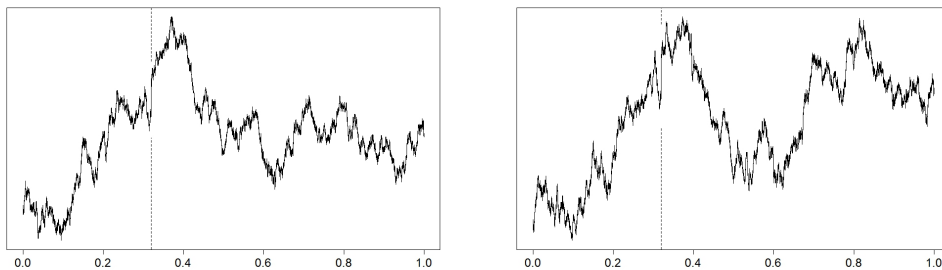
Figure 4: Power of the cojump test in Monte Carlo (2).



*Note: Left plot depicts percentage of realized test statistics (y-axis) against theoretical percentiles of the limit distribution under the hypothesis (x-axis). Right plot gives empirical distribution of test statistics.*

statistical approach combining truncation with spectral covariation estimation and a wild bootstrap test. Our main objective is to infer on cojumps associated with relevant and significant price changes which are very precisely recovered by the method. We have confirmed that the approach is remarkably robust against different values of its block length.

Figure 5: Example of simulated paths in Monte Carlo.



*Note: Dashed segments highlight cojump arrival time.*

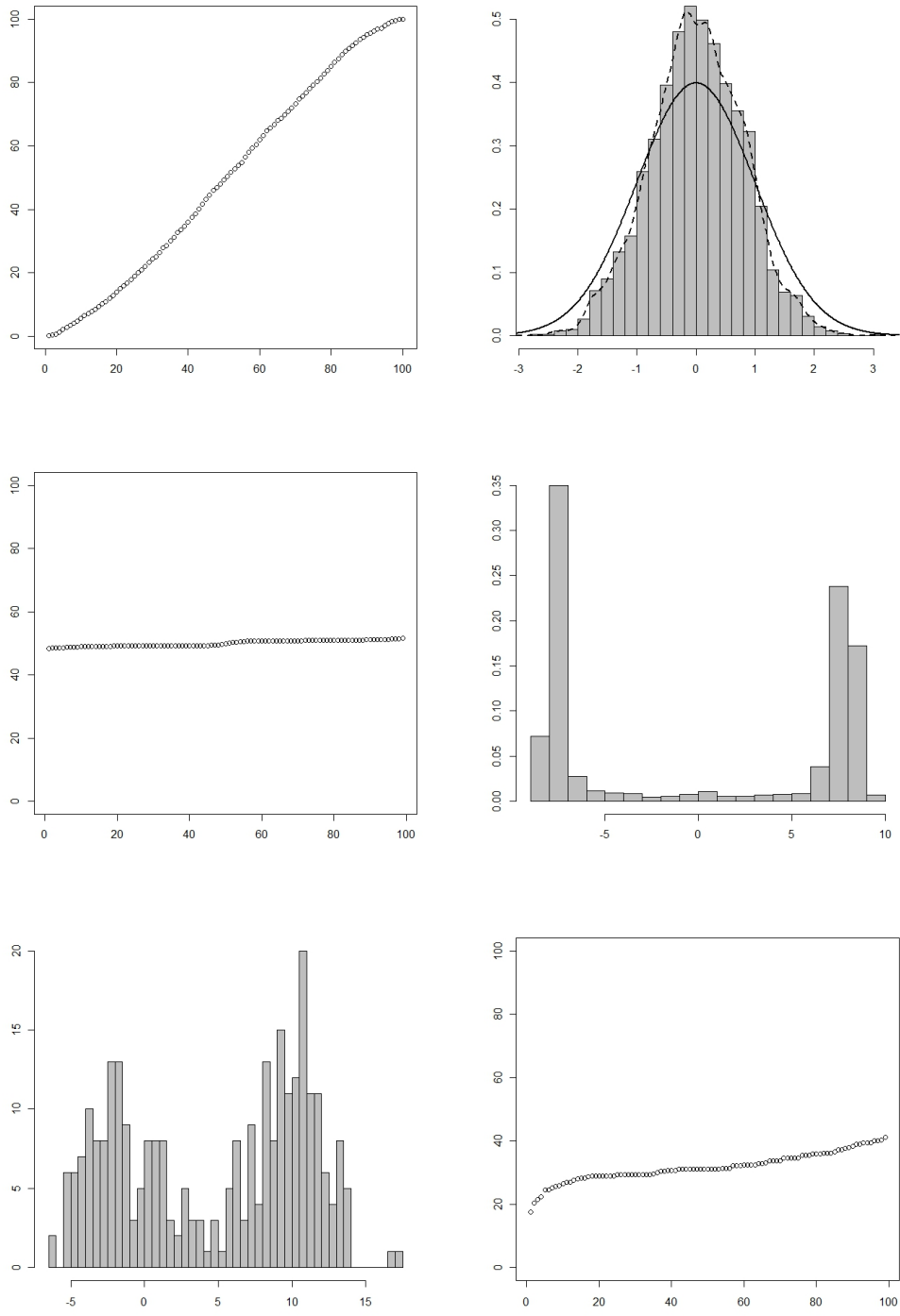


Figure 6: Size and power of cojump test in Monte Carlo,  $h^{-1} = 100$ . Empirical size under hypothesis (top), empirical power under large cojumps (middle) and small cojumps (bottom). Illustrations analogous as above for  $h^{-1} = 33$ .

## References

- Bibinger, M. and Winkelmann, L. (2015), *Econometrics of cojumps in high-frequency data with noise*, 184 (2), 361-378.
- Bibinger, M., Hautsch, N., Malec, P. and Reiß, M. (2014), *Estimating the quadratic covariation matrix from noisy observations: local method of moments and efficiency*, The Annals of Statistics 42 (4), 1312-1346.
- Winkelmann, L., Bibinger, M. and Linzert, T. (2015), *ECB monetary policy surprises: identification through cojumps in interest rates*.